Sediment mobility and connectivity in a catchment: A new mapping approach

Marina Zingaro, Alberto Refice, Emanuele Giachetta, Annarita D'Addabbo, Francesco Lovergine, Vito De Pasquale, Giacomo Pepe, Pierluigi Brandolini, Andrea Cevasco, Domenico Capolongo

PII: S0048-9697(19)31477-9
DOI: https://doi.org/10.1016/j.scitotenv.2019.03.461
Reference: STOTEN 31671

To appear in: *Science of the Total Environment*

Received date: 21 June 2018
Revised date: 25 March 2019
Accepted date: 29 March 2019

Please cite this article as: M. Zingaro, A. Refice, E. Giachetta, et al., Sediment mobility and connectivity in a catchment: A new mapping approach, Science of the Total Environment, https://doi.org/10.1016/j.scitotenv.2019.03.461

Sediment mobility and connectivity in a catchment: a new mapping approach

Marina Zingaro[a], Alberto Refice[b], Emanuele Giachetta[b], Annarita D'Addabbo[b], Francesco Lovergine[b], Vito De Pasquale[c], Giacomo Pepe[d], Pierluigi Brandolini[d], Andrea Cevasco[d], Domenico Capolongo[a]

[a] *Department of Earth and Environmental Sciences, University of Bari, via Orabona 4, 70125 Bari, Italy*
[b] *CNR IREA, via Amendola 122/D, 70126 Bari, Italy*
[c] *Planetek Italia Srl, via Massawa 12, 70132 Bari, Italy*
[d] *Department of Earth, Environmental and Life Sciences, University of Genova, Corso Europa 26, 16132 Genova, Italy*

Corresponding author: Domenico Capolongo, domenico.capolongo@uniba.it

Abstract

In fluvial basin analysis, sediment connectivity is an important element for defining channel dynamics. Nevertheless, although several approaches to quantify this concept have been trialed, there is considerable discussion about ways to measure and assess sediment connectivity. The present study investigates sediment connectivity through the definition of a new index, aiming to integrate functional aspects within a structural component. Our objective is to produce a sediment flow connectivity index (SCI) map, directly applicable to monitoring and management activities. Our SCI is defined as the result of the gradient-based flow accumulation of a sediment mobility index, which is in turn a simple function of rainfall, geotechnical properties of soil and land use. This method is here applied to the Vernazza basin (eastern Liguria, Italy), producing a sediment connectivity map that shows good performance in predicting the positions and accumulation paths of mobilized deposits detected on the ground after the October 25th, 2011, flood event. A further evaluation of the proposed index is performed through a comparison of the maps derived using the SCI and connectivity index (IC) developed by Cavalli et al. (2013), which highlights comparable quantitative overall performances, together with a slightly better qualitative identification of subtle sediment flow paths by the SCI. In spite of current limitations due to, e.g., the local nature of the final index, the availability of input information through open global datasets promises the potential application of this method

to larger-scale assessments, paying attention to properly addressing upscaling and standardization issues.

Keywords: sediment connectivity index, sediment mobility, LIDAR, Vernazza catchment

1. Introduction

Since erosion and deposition processes determine the morphological aspects of a topographic surface and its modifications through time, sediment dynamics are a key process in terms of the source to sink path connectivity, and, in particular, the connection with the fluvial system (Hooke, 2003). For this reason, it becomes fundamental to consider sediment fluxes within a catchment, via a concept more recently referred to as 'sediment connectivity'. Sediment connectivity or (dis) connectivity is affected by, and in turn affects, channel dynamics (Messenzehl et al., 2014; Rinaldi et al., 2016; Surian et al., 2016). Sediment connectivity investigations impose a considerable challenge to the researcher because identification and measurement of sediment fluxes depend on an understanding of the complex nature of internal sediment dynamics in different areas of a catchment system (Bracken and Croke, 2007; Hooke 2003; Fryirs et al., 2007). This spatial variability is a crucial concern in connectivity investigations. Recognition of areas with different degrees of connectivity is helpful for identifying those areas most sensitive to sudden geomorphological modifications, i.e., 'hotspots' (Vergari et al., 2013; Wohl 2014). Hotspot analysis is useful when considering the influence of anthropogenic activities on these processes and, vice versa, the control of these processes on land planning.

The spatial and temporal role of landscape change has been investigated by Doyle and Ensign (2014) and Poeppl and Parson (2017). Multitemporal land connectivity investigations aim to recognize the effects of both natural and anthropogenic drivers through time (Fryirs and Brierley, 2000; Kondolf et al., 2006). Moreover, this concept can be considered at several scales: large-scale assessment of structural connectivity can be undertaken alongside reach-scale studies of functional

connectivity, where research can explore the detailed behavior of sediment pulses (Gran and Czuba, 2017).

Approaches to connectivity have changed over time, through an evolution of concepts, definitions, methods and applications. Early studies introduced the concept of a sediment delivery ratio (Caine and Swanson, 1989), in which a net sediment budget was calculated, represented by the ratio of mass delivered to channels and mass eroded in a catchment. From the sediment yield estimation, geomorphologists then focused on sediment cascades (Fryirs, 2012), i.e., processes (supply, transport, and storage) responsible for sediment movement within a catchment. At a larger scale, the degree of connection among different parts of a landscape (or geomorphic system), e.g., longitudinal, lateral, and vertical connectivity, was argued to be very important (Fryirs, 2012; Wohl, 2014). Others focused on paths and processes differentiation, such as hillslope flows, debris flows, fluvial channels, etc. (Benda, 1990; Benda and Dunne, 1987; Heckmann and Schwanghart, 2013), as well as the location and type of storage landforms (Fryirs et al., 2007). Subsequent papers were concerned with mobilization and remobilization mechanisms (Bracken et al., 2014), micro- and macroscale events (Faulkner, 2008), and anthropogenic impacts (Brierley et al., 2006; Poeppl et al., 2017).

All these studies highlight strong relationships between the so-called structural and functional components of sediment connectivity. In the most accepted definition, *structural connectivity* describes the contiguity of landscape units, while *functional connectivity* describes the interaction among structural elements by geomorphic, hydrological, and ecological processes (Bracken et al., 2014; Turnbull et al., 2008; Wainwright et al., 2011; With et al., 1997). The structural component of connectivity allows one to visualize the spatial distribution of potentially detachable sediment, based on the geomorphic system configuration, while through the functional component, it is possible to gauge the flows of energy and material based on the way catchment processes must be operating. In the past, there have been different ways to measure and analyze sediment connectivity, depending on the consideration of these two components. It must be said that, in the literature, there is some

considerable conflation of structural and functional studies, which makes reviewing the literature challenging. Heckmann et al. (2018) (table 1) have summarized some of these challenges.

There is a need for studies that connect these characteristics to estimate the material fluxes along different compartments of a catchment. Most indices available for connectivity maps are based on the structural component (e.g., Borselli et al., 2008; Cavalli et al., 2013; Crema et al., 2014), whereas applications of models for simulating transport processes connected to the functional component, such as LAPSUS or Caesar-LISFLOOD (Coulthard et al., 2017), are more connected to the modeling of functional connectivity. Tried and tested approaches, such as USLE, RUSLE, or USPED, can sometimes be used for investigations of sediment delivery and connectivity (Capolongo et al., 2008, Aiello et al., 2015). More recently, studies have been identified that attempt to connect the two components (Baartman et al., 2013; Chartin et al., 2017; Hooke et al., 2017; Kalantari et al., 2017). Additionally, several authors have proposed various methods for deriving connectivity maps (Borselli et al., 2008; Cavalli et al., 2013; Ortíz-Rodriguez et al., 2017). However, evaluations of index and model results are, given the complexity of the problem, largely qualitative, and this issue raises the question of how to assess those results in the field.

The need to combine geomorphological structures with sediment dynamics is our starting point to explore connectivity in a catchment. In this study, we propose a new approach for defining and computing a sediment connectivity index, which addresses structural connectivity including functional interactions. Our definitions include a reasonably low number of input variables and data, such as rainfall (as external forcing on the system), land use, geotechnical soil features, and topography (as intrinsic properties). The obtained connectivity map is thus directly applicable to monitoring activities in the study catchment, e.g., for fluvial system understanding and land management. The method is applied to the Vernazza basin (eastern Liguria, Italy), a small river basin characterized by high sediment connectivity and recently affected by an increased frequency of extreme rainfall events (Cevasco et al., 2015). In the following section, we describe in detail our proposed connectivity index, in terms of input data and computational details. In section 3, we introduce the

Vernazza basin in northwestern Italy, where we apply our method, and in section 4, we describe the data processing and validation approach; then, in section 5, we propose an assessment of our connectivity index map with respect to a database of sediment deposits and detachment areas, collected at a fine scale on the ground after a flood event in 2011. We use another well-known connectivity index, the IC index developed by Cavalli et al. (2013), as a benchmark for both qualitative and quantitative evaluations; we also derive a simplified version of our SCI map, spatially smoothed and classified into three levels, suitable for more operational purposes. Finally, in section 6, we critically review our results and, in section 7, we draw some conclusions.

2. Methods

In our study, connectivity is defined as the potential connection among parts of the same system, i.e., the catchment, through sediment transport (Bracken et al., 2014; Wohl, 2014). From this perspective, connectivity is expressed not only by the contiguity between neighboring areas but also by indirect "contact" due to material (sediment and/or water) flow. Mobility and transfer of sediment into the channel network determine sediment fluxes. In our method, we first consider sediment mobilization (erosion) and then the movement of this sediment along pathways toward the main channels and thus to the outlet, considering both longitudinal and lateral linkages. For example, if A and B are two different areas of the catchment, we consider A connected to B if the sediment mobilized in A reaches B. We also assume that the greater the sediment mobility in A, the greater the probability that A is connected with B (Ali et al., 2018) because of the larger availability of sediment to be transported. Furthermore, the path from A to B is determined through a process-based approach, simulating sediment flux through slope-driven flow accumulation. Our sediment connectivity map is based on an estimation of sediment mobility and considers the connection of any cell A in the raster to any other downstream cell through flux patterns determined by flow accumulation. Hence, our sediment flow connectivity index (SCI) measures sediment pathways in lateral and longitudinal directions to the catchment outlet (target).

2.1. Sediment mobility

Sediment mobility is expressed as a product of two factors, namely, one that defines the potential sediment detachment (SM_1) and a second factor that encodes the potential subsequent movement toward surrounding areas, in relation to morphological characteristics of the terrain (SM_2) (fig. 1). The index is derived considering key variables that are the primary factors for starting and supporting sediment transport: morphology, rainfall, and soil and surface characteristics. The combination of these different variables is a consolidated approach in sediment connectivity estimation (Borselli et al., 2008; Cavalli et al., 2013; Chartin et al., 2017; Hook et al., 2017; Lizaga et al., 2018; Wohl et al., 2018).

SM is thus defined as follows:

$$\mathrm{SM} = \mathrm{SM}_1 \cdot \mathrm{SM}_2, \tag{1}$$

with:

$$\mathrm{SM}_1 = \frac{R}{SI}\, L, \tag{2}$$

$$\mathrm{SM}_2 = \frac{S}{Ru}. \tag{3}$$

SM_1 represents the potential availability of detachable sediment in a cell, where *R* is the rainfall index, *SI* is the soil stability index, and *L* is the land use index. The *R* index rates the rainfall amount in a catchment, by assigning high values to areas with greater rainfall and low values to areas with lower rainfall. Rainfall intensity is a proxy of erosivity because it plays a major role in runoff processes and sediment generation (Chartin et al., 2017; Coulthard et al., 2016). *R* is considered a spatially variable index. Its temporal variability determines its role as a simple climatic classification of

territories (if only temporally averaged values are available) or as a forcing element in an event simulation (if more frequent measurements are used). In our SCI index, both uses are potentially envisaged, although in the proposed test application, *R* represents a climatic classification of catchment areas as only annual average rainfall values are available. The *SI* index is determined by considering soil features such as lithology, soil type, permeability, plasticity, and thickness. Soil stability indices are used in other approaches to quantify connectivity, e.g., within USLE-RUSLE indices (Quinoñero-Rubio et al., 2013; Walling and Zhang, 2004) or in other equations (soil loss, curve number, and water and soil erosion models; Grauso et al., 2018a, b; Hooke et al., 2017; Kalantari et al., 2017; Lane et al., 2004, 2009; Mahoney et al., 2018), which, however, do not consider some specific properties, such as soil plasticity and thickness. The inclusion of these soil surface and subsurface characteristics, which are recognized as intrinsic functional properties of connectivity (Heckmann et al., 2018), represents an innovative aspect of the present method. The *SI* index considers stratigraphic and geotechnical properties of soil, through an assessment of water permeability. The land use index *L* is defined, in a similar way to the C-factor used in USLE-RUSLE models (Renard et al., 1997; Whishmeier and Smith, 1978), as a factor that is higher over areas that can favor sediment mobility, i.e., where the soil is more exposed (less protected), e.g., sparsely covered or bare land and is lower in areas with more constrained sediment, e.g., when the soil is covered by vegetation (Borselli et al., 2008), in forests or in urban areas.

Each of these indices is defined as dimensionless, i.e., represented by a scale of normalized value classes or ranges. The definition and ranking of the ranges of numerical intervals for the *R*, *SI* and *L* indices is qualitative and relative to the catchment under study. This approach, though simplified, is used in other definitions of connectivity (e.g., Wohl et al., 2017), as it allows for properly distinguishing areas with different degrees of sediment availability.

The second factor, SM_2, considers the potential sediment movement available from a cell toward the surroundings. Here, *S* is the slope and *Ru* is the ruggedness of the surface (which are both derived from a DEM, similar to, e.g., the IC index by Cavalli et al. (2013)). Various algorithms can be

used to compute the terrain slope (e.g., Schwanghart and Kuhn, 2010); in this case, we use the "D8" approach, where for each cell, the drop/distance ratio from that cell and its eight neighbors is computed, and the maximum slope is selected, which identifies the steepest downhill descent from that cell. Although more sophisticated algorithms exist, this simple method gives an acceptable representation of the steepest descent paths in the case of high-resolution LIDAR topographic data (as those used for this study). Ruggedness describes the topographic variability, defined as the mean difference between a central pixel and its surrounding cells (e.g., Wilson et al., 2007); this simple algorithm is used here to approximate the surface roughness. In fact, a higher local slope can be considered a favorable element for mobility, which is thus modeled as directly proportional to *S*, and vice versa. A greater surface roughness can instead be assumed as an obstacle for sediment displacement, and so, SM_2 is inversely proportional to *Ru*.

The two factors of the final sediment mobility (SM) map thus take into account external forcings (rainfall) and structural (land cover and topography) and functional (soil stability) characteristics of the surface.

2.2. Sediment flow connectivity index

The final connectivity map is defined by a sediment flow connectivity index (SCI) that measures sediment transport through flow accumulation. This map is derived by propagating the SM values, computed as described in the previous section, through a classical flow accumulation algorithm (Schwanghart and Scherler, 2014; Jenson and Domingue, 1988) as follows:

$$\mathrm{SCI} = \log_{10} F(\mathrm{SM}). \tag{4}$$

The flow accumulation algorithm takes into account "potential sediment movement", by sequentially updating the initial raster (SM) map. Conceptually, this process mimics the flow of sedimentary material, which drives available sediment progressively from higher to lower pixels (Ludwig et al.

2007). The flow accumulation procedure, here represented by the function *F*, is often used to estimate the water contributing area of each cell in a catchment. In this ordinary use, unit values of water contributions are often assigned to each cell. In more evolved analyses, spatially variable initial values can instead be used to consider, e.g., the influence of spatial variations of precipitation (Giachetta and Willet, 2018). Such initial seed values are later propagated, from each cell, iteratively across the surface according to a steepest slope principle, so that, at the end of the iterations, terrain cells with the highest flow-accumulated values are those receiving the most contributing flow from the surrounding upslope cells. In our case, assuming that the sediment transport process is similar to that controlling water flow, the SM raster is used to initialize the process, which is then run to represent sediment flow accumulation. We are aware that this method is a simplification regarding sediment transport, both in the detachment-limited and transport-limited regimes of fluvial incision (see, e.g., Gasparini and Brandon, 2011). However, here we are not interested in quantifying the amount of sediment and the processes that are actually moving sediments within channels, nor the erosion/sedimentation rates. Instead, we are merely using the flow accumulation process as a proxy to reconstruct the paths of transported material, following the steepest descent direction principle. This assumption is justified by other studies that use flow accumulation as a proxy for the runoff process in a catchment (see Heckmann et al. (2018) and references therein).

The final map thus obtained shows the sediment pathways in the catchment, in both the lateral (hillslope-channel coupling) and longitudinal (upstream-downstream) direction components, by considering the channel network up to the outlet. The final cell value is thus assumed as a connectivity proxy: a high value indicates that a cell has consistent sediment flow accumulation through flow paths from surrounding upslope cells. As in the case of contributing area maps, the locations with high accumulation are identified with those receiving more contributions, and thus finally with sediment paths.

Our final sediment flow connectivity index thus expresses both the potential availability of detachable sediment as a result of external forcings and landscape characteristics and the connection of this

sediment, through slope-driven flow accumulation processes, in the catchment. A high SCI value in a given terrain cell means a high sediment contribution in that cell from upslope cells, and vice versa, so that the spatial pattern of SCI values reproduces qualitatively the connection paths of sediment throughout the landscape. We note that, as in most other approaches to connectivity mapping (Cavalli et al., 2013, Cossart and Fressard, 2017; Walling and Zhang, 2004), the final values of our SCI have no intrinsic meaning (i.e., they are not physically measurable quantities); the final information lies in the spatial pattern of higher and lower index values.

3. Study area

The proposed method has been applied to the Vernazza basin, a Mediterranean coastal catchment located in the "Cinque Terre" area (eastern Liguria, northwestern Italy). This small mountainous basin (5.7 km^2) has steep slopes and a valley floor occupied by the village of Vernazza, which was built on the final tract of the Vernazza stream (fig. 2a). The geology of the area is structured on a sandstone claystone flysch bedrock (Macigno Formation, Tuscan Unit) and a pelitic complex (Argille e Calcari di Canetolo Formation, Sub-Ligurian Unit), involved in a wide overturned antiform fold (Abbate, 1969; Giammarino and Giglia, 1990). The hillslopes are mainly covered by eluvial–colluvial deposits.

The main characteristics of the catchment are short streams with an ephemeral hydrological regime, slope steepness and a widespread agricultural terraced environment, currently mostly abandoned. Usually, agricultural terraces inhibit connectivity by acting as barriers in the sediment cascade; however, abandoned terraces can reverse this condition, increasing erosion processes (Calsamiglia et al., 2017). According to recent studies performed in the Vernazza basin on the relationships between denudation processes and land use changes (Brandolini et al., 2018a, 2018b; Cevasco et al., 2014, 2013), the lack of maintenance of agricultural terraces makes them susceptible surfaces for sediment mobility because of the deterioration of dry-stone walls and the consecutive intense overland flow. These geomorphological aspects, coupled with the substantial extent of abandoned ter-

races, determine a strong soil instability, mostly during intense rainfall, which occurs during autumn and winter (Brandolini et al., 2018; Cevasco et al., 2015). In past years, this basin has been investigated with regard to the mass wasting processes activated after an extreme rainfall event (occurred on October 25th, 2011) and their correlation with land use (Brandolini et al., 2018a, 2018b; Cevasco et al., 2014; Cevasco et al., 2013; Cevasco and Brandolini, 2015; Galve et al., 2015). These catchment characteristics and the availability of a large quantity of data make the Vernazza basin an ideal test site for applying the proposed sediment connectivity methodology.

4. Data

4.1. Data processing

The following input data were considered for the SCI map. The spatial resolution of all the used maps is 2×2 m^2.

Rainfall data refer to the mean annual precipitation (MAP) recorded by the Liguria rain gauge network and converted to isohyet maps. In particular, MAP values over the Vernazza basin are related to data from the rainfall stations of Levanto, Montale di Levanto, and La Spezia, which are the closest stations, located within 10 km from the Vernazza catchment (Pedemonte, 2005). Due to the topographic gradient and marine influence, there is considerable spatial variability in the rainfall amounts across the catchment, from 1500 mm (1) in the upper basin to 1100 mm (0) in the lower basin.

The isohyet map intervals over the basin were rescaled into index values from 0 to 1 (see table 1 and fig. 2b). In our simplified approach, the maximum value is assumed equal to 1, the minimum value is assumed equal to 0 and the intermediate values correspond to the relatively uniform ranges from 0 to 1. As mentioned above, this arbitrary subdivision has no consequence on the final spatial pattern of connectivity.

The soil stability index values were based on engineering geological units and subunits, mapped by Cevasco et al. (2014), through a lithological and geotechnical soil properties classification. This variable, which constitutes, as already mentioned, a novelty in the approach, comes from many

years of research studies on soil surface characteristics conducted in the Vernazza catchment through field surveys, engineering geological investigations, and laboratory and in situ tests (Cevasco et al., 2014). Units and subunits (sandstone/terraced, sandstone/wild, pelitic/terraced, and pelitic/wild) and their relative soil attributes (e.g., soil type, plasticity, and thickness) allowed us to identify four soil stability classes, to which relative normalized values were assigned (see table 2 and fig. 2c). The rationale of this classification is based on the interpretation of results obtained in a previous study of the catchment (Cevasco et al., 2014).

The land use index values were derived from a land use map, again from Cevasco et al. (2014). As explained in section 2, high values were assigned to classes that can favor sediment detachment (e.g., abandoned terraces), lower values were attributed to land cover classes that were considered obstacles to sediment detachment (e.g., covered soil); urban areas, having virtually null sediment mobility, were assigned a value of 0. The classification is reported in table 3 and in fig. 2d. This type of category ranking for the terrain cover is an approach already tested in a connectivity context (e.g., Wohl et al. 2017).

To apply equations (2) and (3), we processed a DEM of the Vernazza catchment (HR-DTM, 2-m resolution) to derive slope and ruggedness raster maps. We computed ruggedness with the same definition as the TRI (Terrain Ruggedness Index) in Wilson et al. (2007):

$$Ru = \left(\begin{matrix} |z(-1,1) - z(0,0)| + |z(0,1) - z(0.0)| + |z(1,1) - z(0,0)| + |z(-1,0) - z(0,0)| \\ + |z(1,0) - z(0,0)| + |z(1,-1) - z(0,0)| + |z(0,-1) - z(0,0)| + |z(1,-1) - z(0,0)| \end{matrix} \right) \Big/ 8$$

where z is the height of the DTM surface with the positions relative to the central cell (0,0) in a 3×3 analysis window (Wilson et al. 2007). The tool used for TRI calculation was implemented with the "gdaldem" module of the GDAL geospatial software library.

Finally, we used the flow accumulation tool as implemented in the TopoToolbox 2.2 MATLAB® suite (e.g., Schwanghart and Scherler, 2014; Schwanghart and Kuhn, 2010) to propagate the SM values according to the slopes calculated from the DTM, as mentioned above, to obtain the final

SCI map. All the other steps of the procedure, based on mapping, were carried out through ArcMap® and QGIS software.

4.2. Validation approach

The connection between areas within the catchment by sediment transport is thus a complex phenomenon, consisting of dynamic processes, triggered and controlled by many factors. In the previous sections, we have proposed a method for estimating these elements in a static way through an index, but validation of connectivity maps with ground data clearly requires considerable effort in general, and can be considered, in fact, another open question in the scientific community, as quantitatively sensing the processes involved in the concept of connectivity is still at the limit of current technology (Heckmann et al., 2018; Wohl, 2017). As a generalized consensus about validation procedures is yet to be reached, a relatively common approach is to use existing ground data about sediment transfer, typically collected after "bursts" of activity, e.g., following storms or other hazards, as a proxy for the location of sediment transfer processes and pathways. Following this practice, as also adopted by other authors (e.g., Borselli et al., 2008; Cavalli et al., 2013; Wohl et al., 2017), we have compared our SCI map with the distribution of debris flow and mass wasting phenomena, where sediment reached the channel network after an extreme event. We used a detailed landslide inventory map, highlighting channels and hillslopes that presented high connectivity and sediment transfer, realized immediately after the exceptional rainfall event that impacted the easternmost part of the Liguria region and thus the Vernazza basin on October 25th, 2011 (Cevasco et al., 2014), obtained through oblique aerial photointerpretation and field surveys. In view of the abovementioned complexity of the mass wasting processes, we underline again the assumption that such a map of sediment sources and deposition areas can be treated as a proxy to identify potential sediment pathways and sinks. For example, in reference to our concept of connectivity (see section 2), mass wasting deposits can be considered areas (B) that have been reached by the upstream mobilized sediment (A) and are therefore highly connected. We are aware that mass movements can generally also

be a cause of lateral disconnection within a system, but in our case, surface erosion and mass wasting processes are strictly connected with the channel network. In fact, the topography of the study area is characterized by steep and relatively short hillslopes coupled with drainage channels. In such landscapes, the geomorphic processes of mass wasting play a significant role in sediment lateral connectivity (as also argued by Heckmann et al. 2018, section 2.1.3, p. 81). Furthermore, our detailed mass wasting inventory clearly shows that most of the events are laterally connected to the channels.

We also performed a quantitative analysis, using the landslide map as a binary ground truth, and calculating false positive and true positive rates as a function of the SCI index threshold value, represented by a receiver operating characteristic (ROC) curve.

To add objectivity to the validation, the same qualitative and quantitative comparison with ground data was also presented for the connectivity index (IC), developed by Cavalli et al. (2013) and based on the work of Borselli et al. (2008), which was considered here as a benchmark. The two mapping approaches are thus intercompared and evaluated through their respective assessments.

Finally, we presented a simplified version of our SCI map, based on 3-level quantization of a filtered version of the full-resolution map, to foster applications to environmental monitoring and planning.

5. Results

5.1. Mobility and Connectivity Maps

Fig. 2 (e, f) shows the maps for the obtained sediment mobility factors, SM_1 and SM_2, respectively. In the SM_1 map, obtained from equation (2), the catchment areas with a greater mobility index are located in the central part of the catchment and are characterized by the presence of sandstone bedrock covered by eluvial-colluvial deposits (Cevasco et al., 2014), abandoned terraces and medium-high rainfall. Conversely, a smaller mobility index characterizes northern catchment areas, where,

despite a higher rainfall, there is low susceptibility to sediment mobilization, also constrained by the presence of forest coverage.

The SM_2 map, obtained from equation (3), is shown in fig. 2f. By visually comparing the two maps, one can observe that the areas characterized by higher potential sediment availability (SM_1) have medium-high values in the sediment mobility SM_2 map; it can be deduced that the potential sediment detached in a cell can also move from the cell because there are structurally suitable conditions for this movement, thus giving a final high connectivity (see later in the text). Both the SM_1 and SM_2 maps exhibit considerable spatial variations: in the northeastern part, areas with low SM_1 mobility values are more frequent and homogeneous, while in the central and southwestern parts, there are more extensive and widespread areas with medium-high SM_1 mobility. The distribution of SM_2 is more complex, as it also depends on the distribution and variability of the elevations.

The final SCI map, obtained by applying equation (4), is shown in fig. 3. Large values can be observed in the main channels, though variations with lower values along some streams can be observed, possibly indicating spatial differences of flow continuity, related to longitudinal connectivity variations (fig. 3, detailed map on the right). Lower values are, in some cases, also present over the hillslopes, indicating a possibly disconnected flow.

In the northeastern part of the catchment, the SCI is high only along the main channels, which receive sediment contributions from a few upstream areas (a few yellow and several green cells). In the southwestern parts of the basin, there are more high-SCI areas (several yellow and a few green cells), which could be interpreted as areas with a significant potential sediment contribution. Here, larger values would indicate a higher sediment connectivity with “sediment sinks”, i.e., with the main channels. The map also shows that steeper slopes are characterized by different index values in the two basin compartments, i.e., lower SCI in the northeastern part (a few orange and yellow paths) and higher SCI in the southwestern part (more red and orange paths).

5.2. Results validation

We analyzed debris flows, avalanches and landslide sediment paths along eroded gullies, and, in particular, we considered 493 detachment and depositional areas that appear connected with the channels (fig. 4a). The comparison was carried out via qualitative and quantitative analysis. First, through visual interpretation, we observe that displacements and boundaries of the deposit areas, as well as detachment areas, generally correspond to flow paths with higher index values in the connectivity map. These areas are mostly located along the main channels (fig. 4b). This first analysis confirms that the proposed connectivity map generally agrees with the field data and represents indicative sediment patterns, i.e., actual sediment transport paths in the Vernazza basin during the October 25th, 2011, event. The presence of sediment deposits in the channel shows flow connection and sediment supply in the channel reaches. Furthermore, these areas usually terminate in the stream channels for downstream linkages in a connected system. Fig. 5 shows some detailed maps and aerial photographs of areas that clearly exhibit stream channels full of sediment coming from tributary gullies (fig. 5a) or from the steep hillslopes affected by several landslide events whose sediment reached the talweg (figg. 5b, c). Fig. 5b also shows how several of these landslides were triggered on cultivated terrace areas.

As previously mentioned, we also applied quantitative testing, utilizing the mentioned mass wasting source and deposits along eroded gullies as a binary classification reference map, to draw a ROC curve to verify the class recognition capabilities of the connectivity map. The ROC curve for the SCI (fig. 4c) shows a shape that denotes a fair classification capability, with an area under the curve (AUC) corresponding to 0.7.

5.3. Comparison with IC

The IC map of the Vernazza catchment (Borselli et al., 2008; Cavalli et al., 2013) was obtained using the SedInConnect application (release 2.3; Crema and Cavalli, 2018), using as input the same DTM used to compute our SCI map; the impedance factor (W) was assumed to be topography-related (Cavalli et al., 2013) and was computed from the catchment elevation data. The whole IC

map (shown in fig. 6a) shows low connectivity values in the northern basin and medium-high connectivity values in the southwestern areas. The IC map exhibits several features in common with our SCI map (fig. 6b), e.g., the northeastern part of the catchment appears poorly connected with streams, while more high-connectivity areas appear in the southwestern part of the basin. In fig. 5, detailed maps are also shown for the IC map in relation to the field observations.

The ROC curve for IC (fig. 4c) also denotes a fair classification capability, with an AUC of 0.71. In this respect, the performance figures for both the SCI and the IC indices can be considered equivalent for most practical purposes, also considering the mostly overlapping confidence intervals for the two ROC measurements, shown as shaded areas in fig. 4c.

5.4. Sediment connectivity application

The detection of sediment connectivity is important to determine the impact of anthropogenic activities on the basin and, therefore, could be used to devise directives to control the influence of human actions on the fluvial equilibrium.

A map is more applicable as it transmits the principal information through a simple and effective graphic representation. An index map can thus be made more directly applicable through further processing, focused on the particular application context, e.g., reducing the detail by aggregating data over map regions.

The SCI map of the Vernazza basin was thus further postprocessed to better highlight the areas with high, medium and low connectivity. A mean filter was applied using a 9×9 rectangular window, and, then, three classes of values, determined through a natural break index (Jenks), were defined (fig. 7). In this simplified representation, areas characterized by the high connectivity index value class could become observation hotspots in the catchment (in the sense of Vergari et al. (2013) or Wohl (2014), as small areas where the intensity of an event is disproportionately high in relation with the surroundings), e.g., followed over time to detect their evolution, which could reflect geomorphological variations due to, for instance, anthropogenic impacts. This postprocessed map con-

tained most of the original information about sediment flow connectivity (differentiation between two compartments, discontinuous flows, intensity and spatial variations), but, here, contiguous areas with similar connectivity were more evident.

6. Discussion

Our connectivity index is based on local geomorphic, climatic and topographic information. This index allows us to combine functional and structural elements because it considers physical characteristics of the catchment, including surface features (structural component) and the spatial interactions among these elements (functional aspect) by simulating (in a simplified manner) the erosion, deposition and transport processes.

The application of this methodology to the Vernazza basin allows us to distinguish different processes occurring in different catchment compartments. In the northeastern portions of the basin, covered by woods, scrub and meadowlands, a low connectivity index characterizes sediment paths, which indicates lower connection with the stream network. The low values of the connectivity index obtained for this sector of the basin are linked to the key role of natural vegetation cover in decreasing soil depletion and mobility. These results concur with findings reported in the literature about the effect of vegetation on connectivity (Cammeraat et al., 2005; Egozi and Lekach, 2014; Latocha, 2014).

In the central part of the basin, a higher sediment flow connectivity indicates fluxes that are more continuous, determining a higher connectivity of this sector with the main channels. Abandoned agricultural terraces characterize these zones of the catchment. According to preceding studies (mentioned in section 3), these results suggest that terrace abandonment may be considered an important predisposing factor in increasing both the sensitivity to erosion and the transfer of sediment from hillslopes to channels via flows. This aspect is consistent with the extensive literature dealing with the effects of farming terraces on hydrological and geomorphological processes (Calsamiglia et al., 2017; Gerrard and Gardner, 2002; Koulouri and Giourga, 2007; Lasanta et al., 2001; Lesschen et

al., 2008; Tarolli et al., 2014), which reveals how agricultural land abandonment leads to an intensification of geomorphic processes.

Moreover, by observing the obtained map in some detail, one can identify reaches that receive a higher sediment supply through the contribution of the fluxes and their continuity, estimating the whole connectivity pattern: detachment, movement and transport along the surface, and delivery to the channel (fig. 3).

Via a qualitative analysis, based on observation and interpretation of the results, it is possible to denote a general agreement in the description of sediment paths between the SCI index and the IC index developed by Cavalli et al. (2013). The SCI map exhibits a slightly clearer distinction in the central part of the basin, between upper areas (low connectivity, green areas) and lower areas (high connectivity, yellow areas). Furthermore, on a more detailed scale, a larger spatial variation of sediment connectivity in the subbasins can be discerned in the SCI map, compared to the IC map (fig. 5). For instance, in figg. 6c, d, sediment paths are characterized by smaller variations in IC values and wider variations in SCI values, allowing us to better identify variations in sediment flow from upstream to downstream. Another difference between the IC and SCI maps concerns the spatial continuity of connectivity values along channels. In the SCI map, one can identify, along the main channels, some reaches that appear (in darker red) more exposed to sediment supply than the rest of the channel (fig. 5 and figg. 6e, f).

Nevertheless, a quantitative analysis shows that the SCI and IC maps show substantially similar performances when compared to spatial distributions of detachment and mass wasting areas that occurred after a particular event in the Vernazza basin, as also shown by the ROC curves reported in fig. 4. This finding adds confidence to the fact that, although derived from slightly different assumptions and conceptual process models, the two approaches realistically picture sediment connectivity paths in the territory. We are aware that both the SCI and the IC (as well as many of the other indices and/or approaches found in the literature) are basically static maps of terrain features that only mimic the real processes occurring on shorter temporal scales on the ground. In fact, this

is one of the main problems in current research on this subject, as well explained in recent reviews such as Heckmann et al. (2018) and is clearly one of the key aspects that will have to be approached in the near future to reconcile common ground for the various definitions. In this respect, we believe that the quantitative comparison of index maps or model results with field observations for the presence of path connectivity of sediment flows is one viable way to assess and intercompare different methods and approaches.

7. Conclusions

A new method, based on evaluation of climate, topographic, and geomorphological variables, has been presented to derive a sediment connectivity index (SCI) to map sediment flow pathways in a basin. The proposed method combines structural and functional properties to obtain a sediment mobility map, which is then fed to a flow accumulation algorithm, to derive preferential sediment transfer pathways. An interesting novelty of this approach is the application of a soil stability index, based on geotechnical properties of the soil.

The index has been tested in the Vernazza basin, located in eastern Liguria (northwestern Italy), within Cinque Terre National Park, through comparison with a map of mass waste sources and deposits, compiled after ground inspections following a flood event that occurred on Oct. 25, 2011. Results show that the index identifies high efficiency areas of sediment flows, locating those characterized by high sediment connectivity in potential so-called hotspot areas. A comparison between the proposed SCI and the sediment connectivity index (IC) proposed by Cavalli et al. (2013) denotes comparable quantitative performances of the two indices at the local scale (ROC curves with very similar AUC values), with the SCI exhibiting slightly larger local spatial variations of connectivity values and a somewhat better identification of spatial continuity in the sediment connectivity. We must underline that, in this case study, all the input parameters for the SCI have been used in a static fashion, i.e., without considering their variability in time, although at least the climatic fac-

tors, such as rainfall, could easily be considered temporally variable, and thus potentially provide better performance in adaptively modeling particular events.

This quantitative validation exercise, although inevitably based on assumptions and approximations, especially regarding the not physically measurable quantities used as a proxy for sediment connectivity, is one of the innovative aspects of our work and constitutes, in our view, a viable means to test performances of newly proposed approaches to connectivity mapping. Furthermore, the fine-scale assessment applied to the Vernazza catchment can also be considered a novelty in the sediment connectivity framework.

On the other hand, the present approach has limitations. The first one is given by the combination of structural and functional components of connectivity, i.e., the new index tries to integrate a functional aspect within a structural connectivity index, through feeding a sediment mobility map within a flow accumulation algorithm, to describe the flow processes of sediment in a catchment; however, this method still does not constitute a true, physically based interaction model of the two components. A second limitation is the local character of the new approach, i.e., since input variables are considered mostly adimensional indices, numerical values of the final SCI index are also indicative and depend on the area to which the method is applied; in our case, the index has been calibrated and validated in the Vernazza catchment as a proof of concept. This method means that intercomparisons across different areas would require, e.g., some normalization of values. Overcoming this limitation, which is also common to many other current approaches to connectivity mapping through indices, would require expressing all the input variables in terms of standardized, physically based or probabilistic quantities. For development of the SCI index and its wider application, a greater amount of empirical data collected in the field is required to establish factor values in a weighting procedure. This need constitutes an interesting path for future research.

Our approach could be further improved, e.g., to obtain more accuracy or to consider other possible variables, such as different parameters for evaluating soil stability (clay fraction, organic carbon

weight, etc.), location and properties of structures considered barriers or preferred paths for connectivity (e.g., weirs, embankments, etc.).

The proposed mapping approach could also be directed, with proper upscaling adaptations, toward the use of parameters (rainfall, soil units, land use, and morphological aspects) that are considered available on a global scale, e.g., utilizing open global data sets, which are increasingly updated and completed. This addition is in fact one of the planned future developments of the proposed methodology.

Acknowledgements

This research was supported by the contribution of the PON FSE-FESR Research and Innovation 2014-2020 for Innovative and Industrial PhDs, from which Marina Zingaro was funded. The authors thank two anonymous reviewers for the insightful comments that helped improve the article quality.

References

Abbate E., 1969. Geologia delle Cinque Terre e dell'entroterra di Levanto (Liguria orientale). Memorie della Società Geologica Italiana 8, 923-1014.

Aiello A., Adamo M., Canora F., 2015. Remote sensing and GIS to assess soil erosion with RUSLE3D and USPED at river basin scale in southern Italy. Catena 131, 174-185.

Ali G., Oswald C., Spence C., Wellen C., 2018. The T-TEL Method for Assessing Water, Sediment, and Chemical Connectivity. Water Resources Research 54, 634–662.

Baartman J.E.M., Masselink R., Keesstra S.D., Temme A.J.A.M., 2013. Linking Landscape morphological complexity and sediment connectivity. Earth Surf. Process. Landf. 38, 1457-1471.

Benda L., 1990. The influence of debris flows on channels and valley floors in the Oregon coast range, USA. Earth Surf. Process. Landf. 15, 457-466.

Benda L., Dunne T., 1987. Sediment routing by debris flow. Erosion and Sedimentation in the Pacific Rim. IAHS 165, 213-223.

Borselli L., Cassi P., Torri D., 2008. Prolegomena to sediment and flow connectivity in the landscape: A GIS and field numerical assessment. Catena 75, 268-277.

Bracken L.J., Croke J., 2007. The concept of hydrological connectivity and its contribution to understanding runoff-dominated geomorphic systems. Hydrol. Process. 21, 1749-1763.

Bracken L.J., Turnbull L., Wainwright J., Bogaart P., 2014. Sediment connectivity: a framework for understanding sediment transfer at multiple scales. Earth Surf. Process. Landf. https://doi.org/10.1002/esp.3635.

Brandolini P., Cevasco A., Capolongo D., Pepe G., Lovergine F., Del Monte M., 2018a. Response of terraced slopes to a very intense rainfall eventand relantionship with land abandonment: a case study from Cinque Terre (Italy). Land Degrad. Develop. 29, 630-642. https://doi.org/10.1002/ldr.2672.

Brandolini P., Pepe G., Capolongo D., Cappadonia C., Cevasco A., Conoscenti C., Marsico A., Vergari F., Del Monte M., 2018b. Hillslope degradation in representative Italian areas: just soil erosion risk or opportunity of development? Land Degrad. Develop. https://doi.org/10.1002/ldr.2999.

Brierley G., Fryirs K., Jain V., 2006. Landscape connectivity: the geographic basis of geomorphic applications. Area 38(2), 165-174.

Burrough P.A., McDonell R.A., 1998. Principles of Geographical Information Systems, Oxford University Press, New York.

Caine N., Swanson F.J., 1989. Geomorphic coupling of hillslope and channel systems in two small mountain basins. Z. Geomorphol. 33, 189-203.

Calsamiglia A., Fortesa J., Garcia-Comendador J., Lucas-Borja M.E., Calvo-Cases A., Estrany J., 2017. Spatial patterns of sediment connectivity in terraced lands: Anthropogenic controls of catchment sensitivity. Land Degrad Dev. https://doi.org/10.1002/ldr.2840.

Cammeraat E, van Beek R, Kooijman A., 2005. Vegetation succession and its consequences for slope stability in SE Spain. Plant and Soil 278: 135-147. https://doi.org/10.1007/s11104-005-5893-1.

Capolongo D., Pennetta L., Piccarreta M., Fallacara G., Boenzi F., 2008. Spatial and temporal variations in soil erosion and deposition due to land-levelling in a semi-arid area of Basilicata (Southern Italy). Earth Surf. Process. Landf. 10, 364-379.

Cavalli M., 2017. Geomorphometric approaches to assess sediment connectivity and geomorphic changes in mountain catchments, Workshop ″Monitoraggio e valutazione dei processi erosivi″, Roma, 22/6/2017.

Cavalli M., Tarolli P., Marchi L., Dalla Fontana G., 2008. The effectiveness of airborne LiDAR data in the recognition of channel-bed morphology. Catena 73, 249-260.

Cavalli M., Trevisani S., Comiti F., Marchi L., 2013. Geomorphometric assessment of spatial sediment connectivity in small Alpine catchments. Geomorphol. 188, 31-41.

Cavalli M., Tarolli P., Dalla Fontana G., Marchi L., 2016. Multi-temporal analysis of sediment source areas and sediment connectivity in the Rio Cordon catchment (Dolomites), Rend. Online Soc. Geol. It. 39, 27-30.

Cevasco A., Brandolini P., Scopesi C., Rellini I., 2013. Relationships between geo-hydrological processes induced by heavy rainfall and land-use: the case of 25 October 2011 in the Vernazza catchment (Cinque Terre, NW Italy). J Maps 9(2), 289–298. https://doi.org/10.1080/17445647.2013.780188.

Cevasco A., Pepe G., Brandolini P., 2014. The influences of geological and land use settings on shallow landslides triggered by an intense rainfall event in a coastal terraced environment. Bull Eng Geol Environ. 73, 859-875.

Cevasco A., Diodato N., Revellino P., Fiorillo F., Grelle G., Guadagno F.M., 2015. Storminess and geo-hydrological events affecting small coastal basins in a terraced Mediterranean environment. Sci Total Environ 532, 208-219. https://doi.org/10.1016/j.scitotenv.2015.06.017.

Cevasco A, Brandolini P., 2015. Rapid debris volume estimation by LiDAR data derived DEMs: applications to the 25 October 2011 debris flood event at Vernazza (Cinque Terre, Italy). Rendiconti Online della Società Geologica Italiana 35: 62-65.

Chartin C., Evrard O., Laceby J.P., Onda Y., Ottlé C., Lefèvre I., Cerdan O., 2017. The impact of typhoons on sediment connectivity: Lessonslearnt contaminated coastal catchments of the Fukushima Prefecture (Japan). Earth Surf. Process. Landf. 42, 306-317.

Cossart E., Fressard M., 2017. Assessment of structural sediment connectivity within catchments: Insighs from graph theory. Earth Surface Dynamics 5 (2), 253-268.

Coulthard T.J., Van De Wiel M.J., 2017. Modelling long term basin scale sediment connectivity, driven by spatial land use changes. Geomorphol. 277, 265-281.

Crema S., Schenato L., Goldin B., Marchi L., Cavalli M., 2014. Toward the development of a stand-alone application for the assessment of sediment connectivity, Rend. Online Soc. Geol. Ital. 34, 58-61.

Crema, S., and Cavalli, M., 2018. SedInConnect: A stand-alone, free and open source tool for the assessment of sediment connectivity. *Computers & Geosciences*, *111*, 39-45.

Doyle M.W., Ensign S.H., 2014. Alternative Reference Frames in River System Science. BioScience 59, 6, 499-510.

Egozi R, Lekach J., 2014. Stream catchment dynamics. Geomorphol. 212, 1-3. doi: 10.1016/j.Geomorphol.2013.12.003

Faulkner H., 2008. Connectivity as a crucial determinant of badland morphology and evolution. Geomorphol. 100, 91-103.

Fryirs K., Brierley G., 2000. A geomorphic approach to the identification of river recovery potential. Physical Geography 21(3), 244-277.

Fryirs K., 2012. (Dis)connectivity in catchment sediment cascades: a fresh look at the sediment delivery problem. Earth Surf. Process. Landf. 38, 30-46.

Fryirs K., Brierly G., Preston N., Kasai M., 2007. Buffers, barriers and blankets: The (dis)connectivity of catchment-scale sediment cascades. Catena 70, 49-67.

Gasparini, N.M., Brandon, M.T., 2011. A generalized power law approximation for fluvial incision of bedrock channels. Journal of Geophysical Research: Earth Surface 116, 1–16. https://doi.org/10.1029/2009JF001655.

Gay A., Cerdan O., Mardhel V., Desmet M., 2016. Application of an index of sediment connectivity in a lowland area. J. Soils Sediments 16 (1), 280-293.

Gerrard J, Gardner R., 2002. Relationships between landsliding and land use in the Likhu Khola drainage basin, Middle Hills, Nepal. Mountain Research and Development 22, 48-55. https://doi.org/10.1659/0276-4741(2002)022[0048:RBLALU]2.0.CO;2.

Giachetta E., Willet S.D., 2018. A global dataset of river network geometry. Nature Scientific data 5, 180127. https://doi.org/10.1038/sdata.2018.127.

Giammarino S, Giglia G., 1990. Gli elementi strutturali della piega di La Spezia nel contesto geodinamico dell'Appennino Settentrionale. Bollettino della Società Geologica Italiana 109, 683–692.

Gran K.B., Czuba J.A., 2017, Sediment pulse evolution and the role network structure. Geomorphol. 177, 17-30.

Grauso S., Pasanisi F., Tebano C., 2018a. Assessment of a Simplified Connectivity Index and Specific Sediment Potential in River Basins by Means of Geomorphometric Tools. Geosciences 8, 48-62.

Grauso S. Pasanisi F., Tebano C., Grillini M., Peloso A., 2018b. Investigating the Sediment Yield Predictability in Some Italian Rivers by Means Hydro-Geomorphometric Variables. Geosciences 8, 249-268.

Heckmann T., Schwanghart W., 2013. Geomorphic coupling and sediment connectivity in an alpine catchment-Exploring sediment cascades using graph theory. Geomorphol. 182, 89-103.

Heckmann T., Cavalli M., Cerdan O., Foerster S., Javaux M., Lode E., Smetanová A., Vericat D., Brardinoni F., 2018. Indices of sediment connectivity: opportunities, challenges and limitations. Earth-Science Reviews 187, 77-108.

Hooke J., 2003. Coarse sediment connectivity in river channel systems: a conceptual framework and methodology. Geomorphol. 56, 79–94.

Hooke J.M., Sandercock P., Cammeraat L.H., Lesschen J.P., Borselli L., Torri D., Meerkerk A., van Wesemael B., Marchamalo M., Gonzalo B., Boix-Fayos C., Castillo V., Navarro-Cano J.A., 2017. Mechanism of degradation and identification of connectivity and erosion hotspots. In Combating desertification and land degradation, Hooke J., Sandercock P. (eds). Springer International Publishing, 13-37.

Jenson S.K., Domingue J.O., 1988. Extracting topographic structure from digital elevation data for geographic information System analysis. Photogrammetric Engineering and Remote Sensing 14, 1593-1600.

Kalantari Z., Cavalli M., Cantone C., Crema S., Destouni G., 2017. Flood probability quantification for road infrastructure: Data-driven spatial-statistical approach and case study applications. Sci. Total Environ. 581-582, 386-398.

Koulouri M, Giourga C., 2007. Land abandonment and slope gradient as key factors of soil erosion in Mediterranean terraced lands. Catena 69, 274-281. https://doi.org/10.1016/j.catena.2006.07.001.

Lane S.N., Brookes C.J., Kirkby M.J., Holden J., 2004. A network-index-based version of TOPMODEL for use with high-resolution digital topographic data. Hydrol. Process. 18 (1), 191-201.

Lane S.N., Reaney S.M., Heathwaite A.L., 2009, Representation of landscape hydrological connectivity using a topographically driven surface flow index. Water Resources Research 45 (8), W08423.

Lasanta T, Arnáez J, Oserin M, Ortigosa LM., 2001. Marginal lands and erosion in terraced fields in the Mediterranean mountains. A Case Study in the Camero Viejo (Northwestern Iberian System,

Spain). Mountain Research and Development 21, 69-76. https://doi.org/10.1659/0276-4741(2001)021[0069:MLAEIT]2.0.CO;2.

Latocha A., 2014. Geomorphic connectivity within abandoned small catchments (Stołowe Mts, SW Poland). Geomorphol. 212, 4-15. https://doi.org/10.1016/j.geomorph.2013.04.030.

Lesschen JP, Cammeraat LH, Nieman T., 2008. Erosion and terrace failure due to agricultural land abandonment in a semi-arid environment. Earth Surface Processes and Landforms 33: 1574-1584. https://doi.org/10.1002/esp.1676.

Lizaga I., Quijano L., Palazón L., Gaspar L., Navas A., 2018. Enhancing connectivity index to assess the effects of land use changes in a mediterranean catchment. Land Degrad. Develop. 42, 1588-1596. https://doi.org/10.1002/esp.4321.

Ludwing J.A., Bastin G.N., Chewings V.H. Eager R.W., Liedloff A.C., 2007. Leakiness: a new index for monitoring the health of arid and semiarid landscapes using remotely sensed vegetation cover and elevation data. Ecol. Indic. 7, 442-454.

Mahoney D.T., Fox J.F., Al Aamery N., 2018. Watershed erosion modelling using the probability of sediment connectivity in a gently rolling system. Hydrol. 561, 862-883.

Messenzehl K., Hoffmann T., Dikau R., 2014. Sediment connectivity in the high-alpine valley of Val Müschauns, Swiss National Park-linking geomorphic field mapping with geomorphometric modelling. Geomorphol. 221, 215-229.

Ortíz-Rodrígez A.J., Borselli L., Sarocchi D., 2017. Flow connectivity in active volcanic areas: Use of index of connectivity in the assessment of lateral flow contribution to main streams. Catena 157, 90-111.

Pedemonte, R., 2005. Contributo alla classificazione dei climi della Liguria. Distribuzione geografica delle precipitazioni annue – IV parte. Rivista Ligure di Meteorologia 16 (anno V). Società Meteorologica Italiana – Sezione Liguria.

Poeppl R.E., Keesstra S.D., Maroulis J., 2017. A conceptual connectivity framework for understanding geomorphic change in human impacted fluvial systems. Geomorphol. 277, 237-250.

Poeppl R.E., Parson A.J., 2017. The geomorphic cell: a basis for studying connectivity. Earth Surf. Process. Landf. 43, 1155-1159.

Quinoñero-Rubio J.M., Boix-Fayos C., de Vente J., 2013. Desarollo y applicacion de un indice multifactorial de connectividad de sedimentos a escala de cuenca: Development and application of a multifactorial sediment connectivity index on the catchment scale (in Spanish). Cuadernos de Investigación Geográfica 39 (2), 203-223.

Renard, K.G., Foster, G.R., Weesies, G.A., Mccool, D.K., Yoder, D.C., 1997. Predicting Soil Erosion By Water: a Guide to Conservation Planning with the Revised Universal Soil Loss Equation (RUSLE). U.S. Department of Agriculture, Agriculture Handbook No. 703.

Righini M., Surian N., 2018. Remote sensing as a toll for analysing channel dynamics and geomorphic effects of floods. In: Refice A., D'Addabbo A., Capolongo D. (Eds.) Flood Monitoring through Remote Sensing. Springer Remote Sensing/Photogrammetry. Springer, Cham, 27-59.

Rinaldi M., Surian N., Comiti F., Bussettini M., 2016. Sistema di valutazione idromorfologica, analisi e monitoraggio dei corsi d'acqua, Roma.

Rinaldi M., Amponsah W., Benvenuti M., Borga M., Comiti F., Lucía A., Marchi L., Nardi L., Righini M., Surian N., 2016. An integrated approach for investigating geomorphic response to extreme events: methodological framework and application to the October 2011 flood in the Magra River catchment, Italy, Earth Surf. Process. Landf. 41, 835-846.

Schwanghart W., Kuhn N.J., 2010. TopoToolbox: a set of MATLAB functions for topographic analysis. Environmental Modelling and Software. 25, 6, 770-781. doi: 10.1016/j.envsoft.2009.12.002

Schwanghart W, Scherler D., 2014. Short Communication: TopoToolbox 2 – MATLAB-based software for topographic analysis and modeling in Earth surface sciences. Earth Surface Dynamics 2, 1–7. https://doi.org/10.5194/esurf-2-1-2014.

Schneevoigt N.J., van der Linden S., Thamm H.P., Schrott L., 2008. Detecting Alpine landforms from remotely sensed imagery. A pilot study in the Bavarian Alps. Geomorphol. 93 (1-2), 104-119.

Surian N., Righini M., Lucía A., Nardi L., Amponsah W., Benvenuti M., Borga M., Cavalli M., Comiti F., Marchi L., Rinaldi M., Viero A., 2016. Channel response to extreme floods: Insights on controlling factors from six mountain rivers in northern Apennines, Italy, Geomorphol. 272, 78-91.

Tarolli, P., Preti, F., Romano, N., 2014. Terraced landscapes: From an old best practice to a potential hazard for soil degradation due to land abandonment. *Anthropocene*, *6*, 10-25.

Turnbull L., Wainwright J., Brazier R. E., 2008. A conceptual framework for understanding semi-arid land degradation: ecohydrological interactions across multiple-space and time scales. Ecohydrol. 1, 23-34.

Vergari F., Della Seta M., Del Monte M., Barbieri M., 2013. Badlands denudation "hot spots": The role of parent material properties on geomorphic processes in 20-years monitored sites of Southern Tuscany (Italy). Catena 106, 31-41.

Wainwright J., Turnbull L., Ibrahim T.G., Lexartza-artza I., Thornton S.F., Brazier R.E., 2011. Linking environmental regimes, space and time: Interpretations of structural and functional connectivity. Geomorphol. 126, 387-404.

Walling D.E., Zhang Y., 2004. Predicting slope-channel connectivity: a national-scale approach. IAHS Publ. 288, 107-114.

Wischmeier, W.H., Smith, D.D., 1978. Predicting rainfall erosion losses - a guide to conservation planning., Predicting rainfall erosion losses - a guide to conservation planning. USDA, Science and Education Administration.

Wilson M.F.J., O'Connell B., Brown C., Guinan J.C., Grehan A.J., 2007. Multiscale terrain analysis of multibeam bathymetry data for habitat mapping on the continental slope. Marine Geodesy. 30, 3-35.

With K.A., Gardner R.H., Turner M.G., 1997. Landscape connectivity and population distributions in heterogeneous environments. Oikos 78, 151-169.

Wohl E., 2014. Rivers in the landscape. Science and management, Oxford.

Wohl E., 2017. Connectivity in rivers. Prog. Phys. Geogr. 41 (3), 345-362.

Wohl E., Rathburn S., Chignell S., Garrett K., Laurel D., Livers B., Patton A., Records R., Richards M., Schook D.M., Sutfin N.A. Wegener P., 2017. Mapping longitudinal stream connectivity in the North St. Vrain Creek watershed of Colorado. Geomorphol. 277, 171-181.

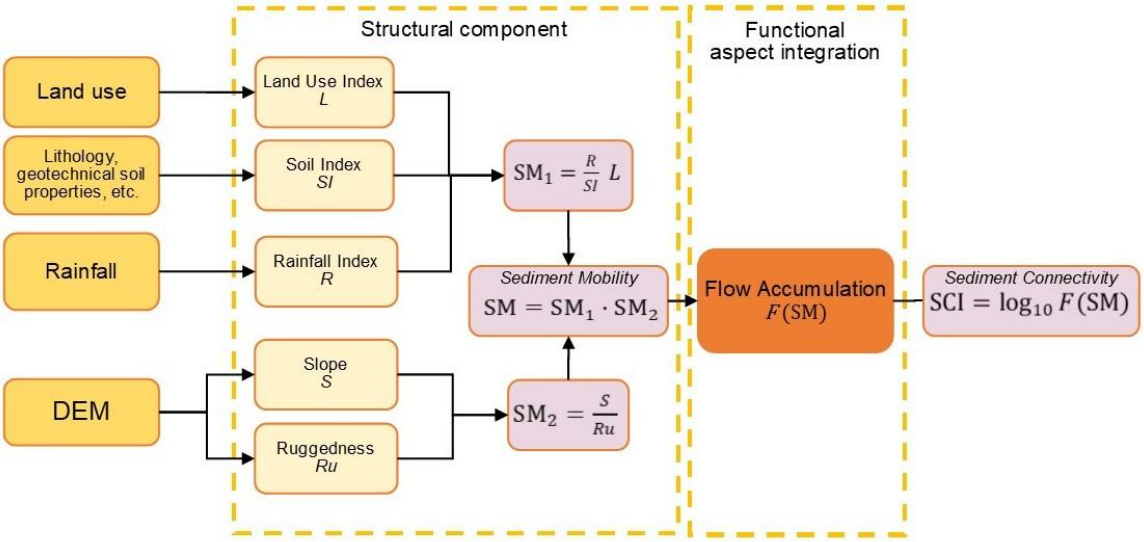

Figure 1. Processing sequences of the proposed mapping approach for sediment connectivity. Sediment Mobility is derived from two factors (SM_1 and SM_2). In SM_1, *R* is Rainfall, *SI* is the Soil stability index, and *L* is the Land use index. In SM_2, *S* is Slope and *Ru* is Ruggedness. Sediment Flow Connectivity (SCI) is obtained as the logarithm of the SM flow result. See text for further details.

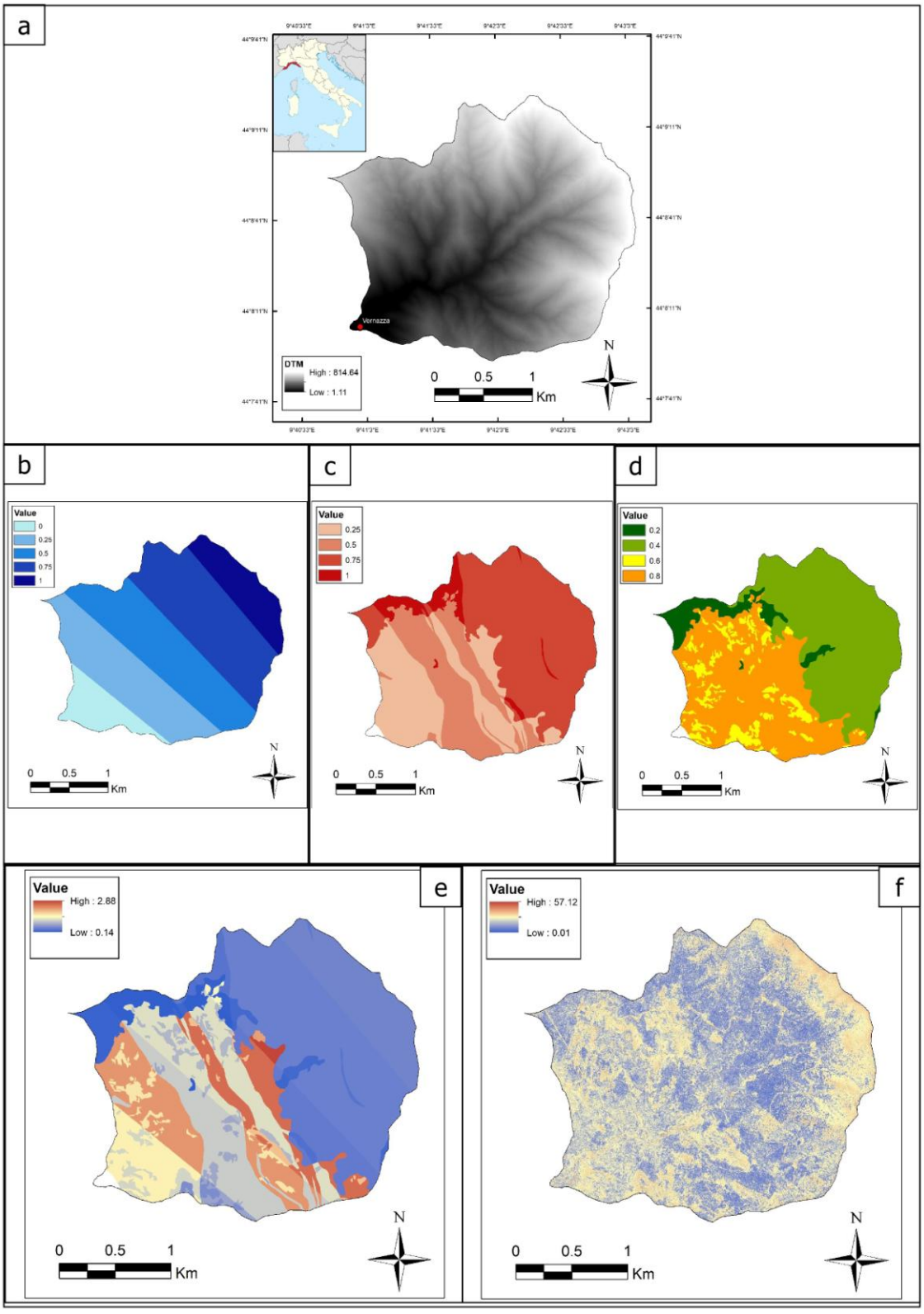

Figure 2. a. DTM of the Vernazza basin in the eastern Liguria region (northwestern Italy). **b**, **c**, **d**. Sediment mobility ground data maps for the Vernazza basin: rainfall data (a): isohyets of the Vernazza basin in the value classes (Mean Annual Precipitation); soil stability data (b): engineering geological units in assigned value classes (engineering geological map from Cevasco et al. (2014)); land use data (c) in associated value classes (land use map from Cevasco et al. (2014)). In b and c, urban areas are masked. **e, f**. Sediment mobility factors: SM_1 map (e); SM_2 map (f).

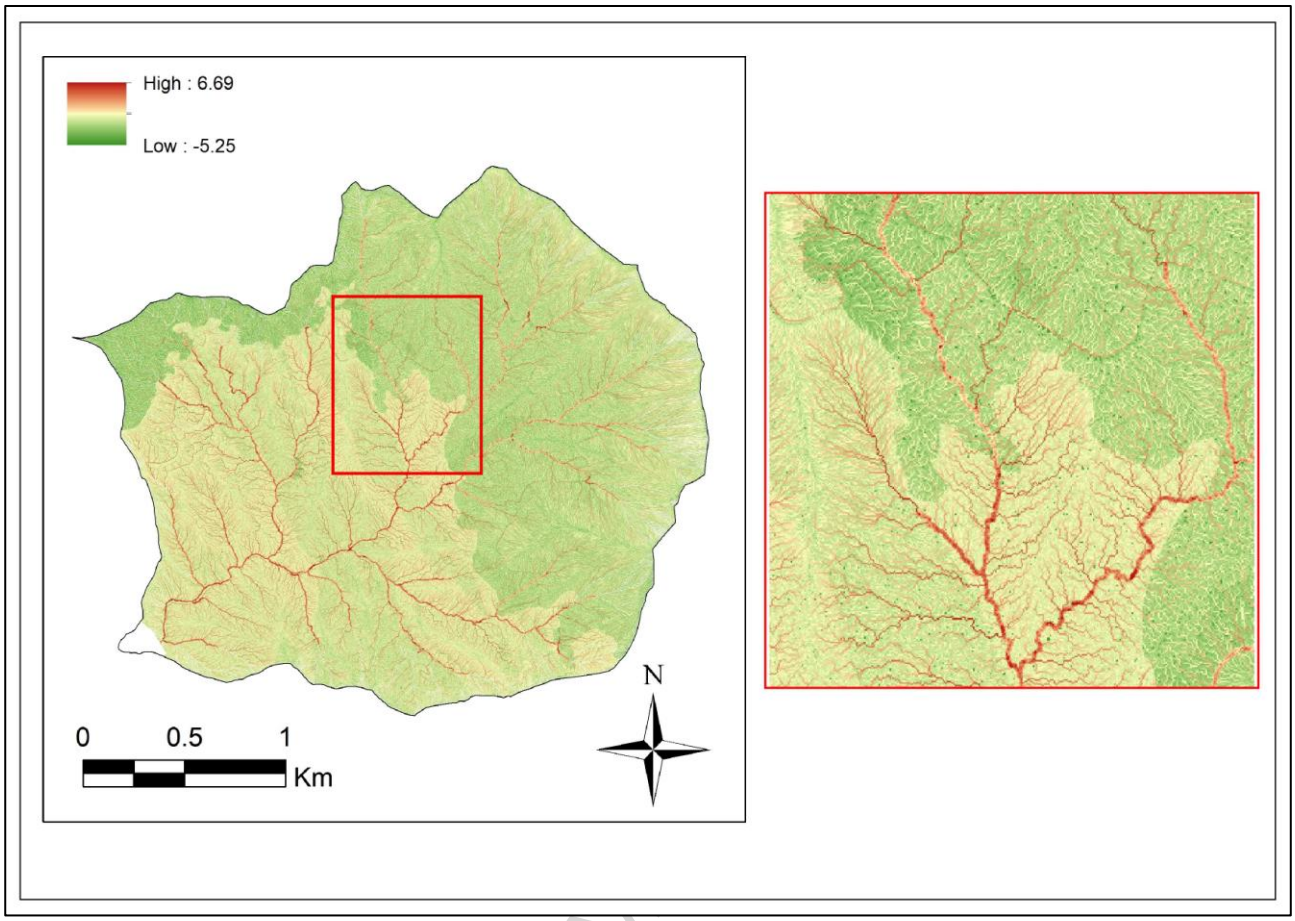

Figure 3. Left: sediment connectivity index (SCI) map of the Vernazza basin. Right: detailed map corresponding to the red box on the left, illustrating examples of different connectivity values and flow discontinuities along the main channels.

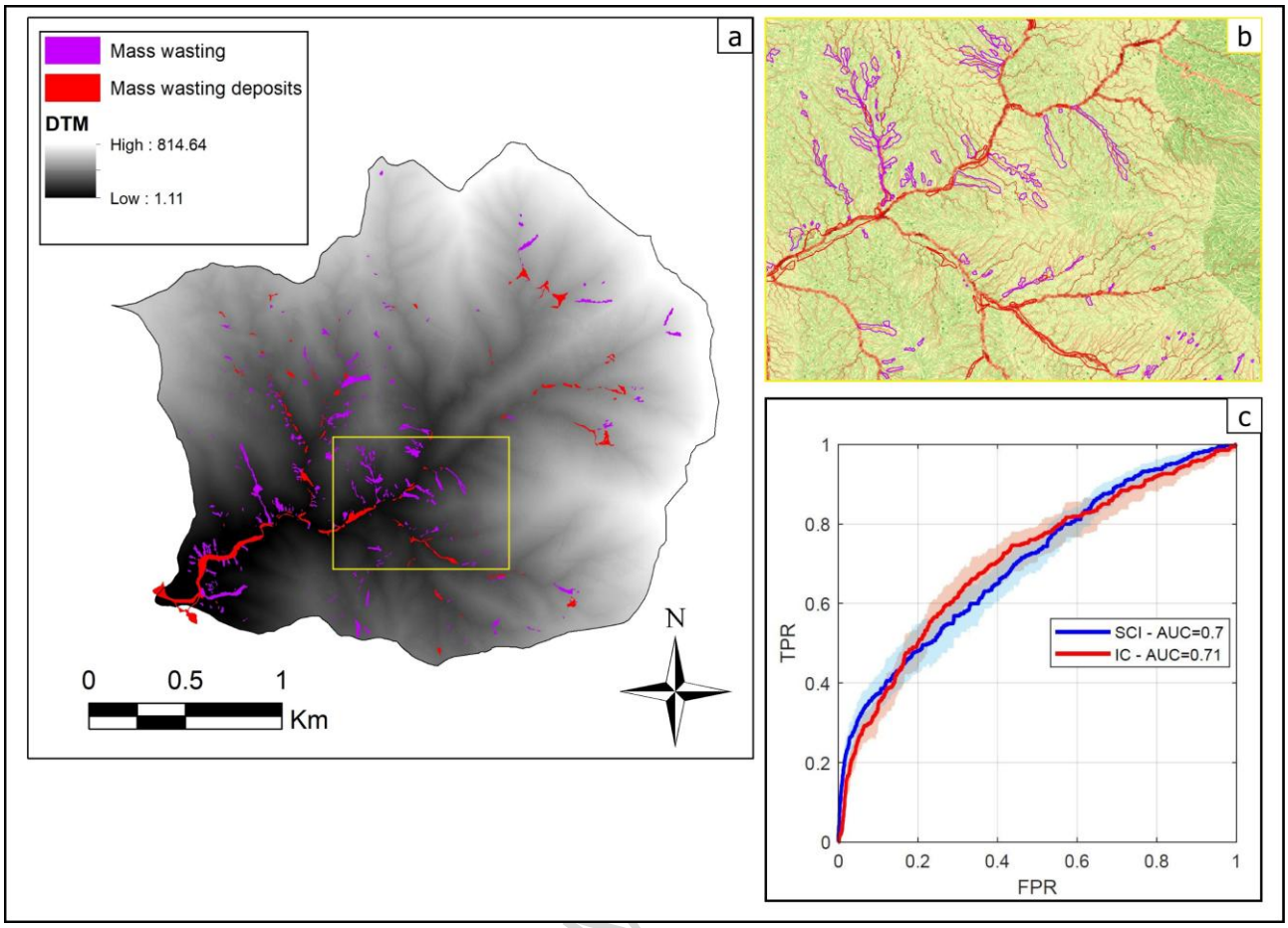

Figure 4. a. Mass wasting and deposits triggered by the event on October 25th, 2011, overlaid on a DTM height map. **b.** Detail in the yellow rectangle in a., overlaid on the SCI map (color scale as in fig. 3). **c.** ROC (Receiver Operating Characteristic) curves computed by plotting the True Positive Rate (TPR) and the False Positive Rate (FPR), with respect to the binary map in panel a, for the proposed SCI and IC indices. Shaded areas indicate confidence intervals computed through a bootstrap procedure. Areas under the curve (AUC) for both plots are indicated.

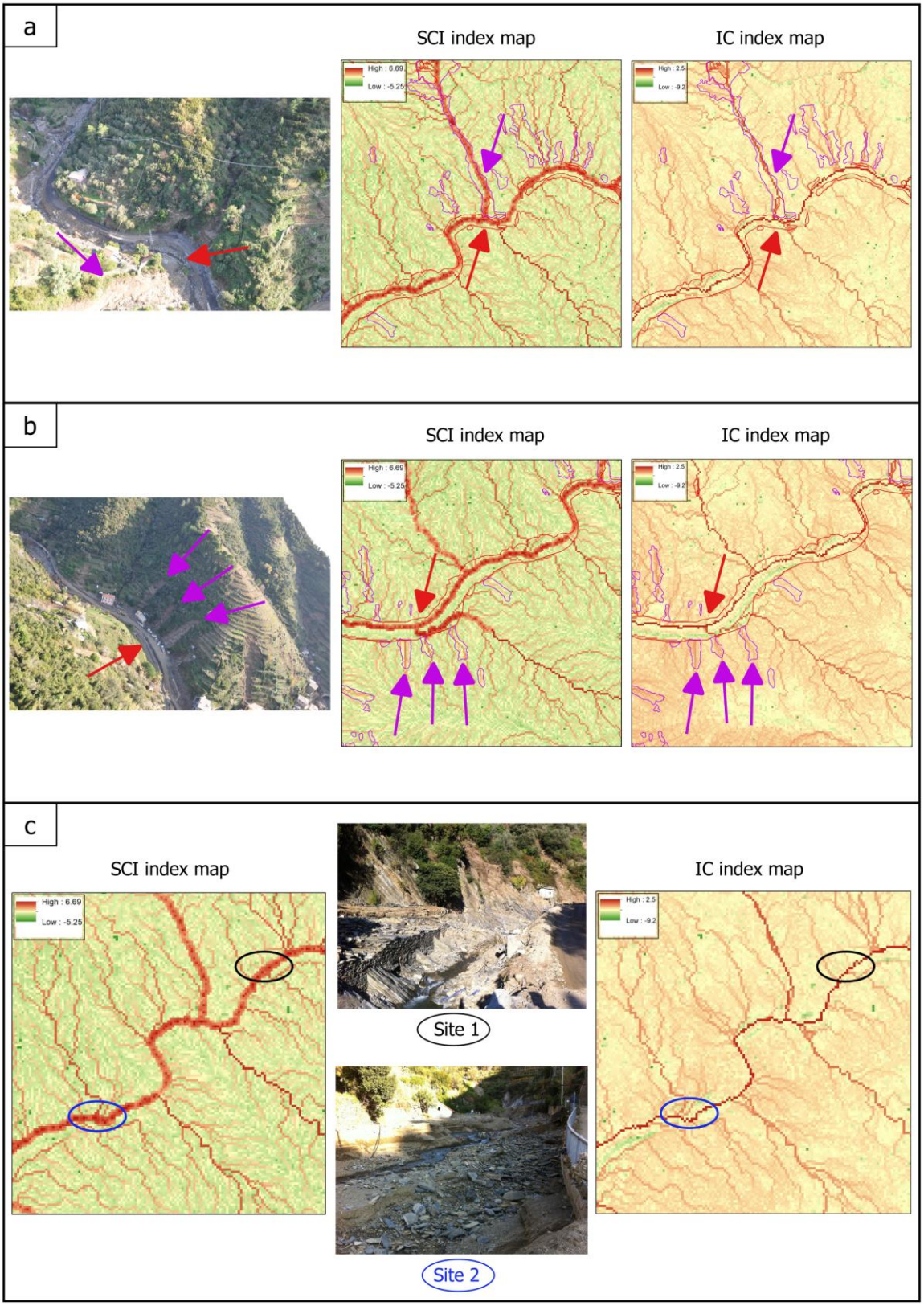

Figure 5. Sample areas of the Vernazza basin with high SCI values, coinciding with (**a**, **b**) detachment and deposition areas in the field and (**c**) channel reaches characterized by sediment deposits. For comparison, IC maps for the same areas are also shown. Helicopter images are courtesy of Comando unità CARabinieri per la tutela forestale, AMBientale e Agroalimentare.

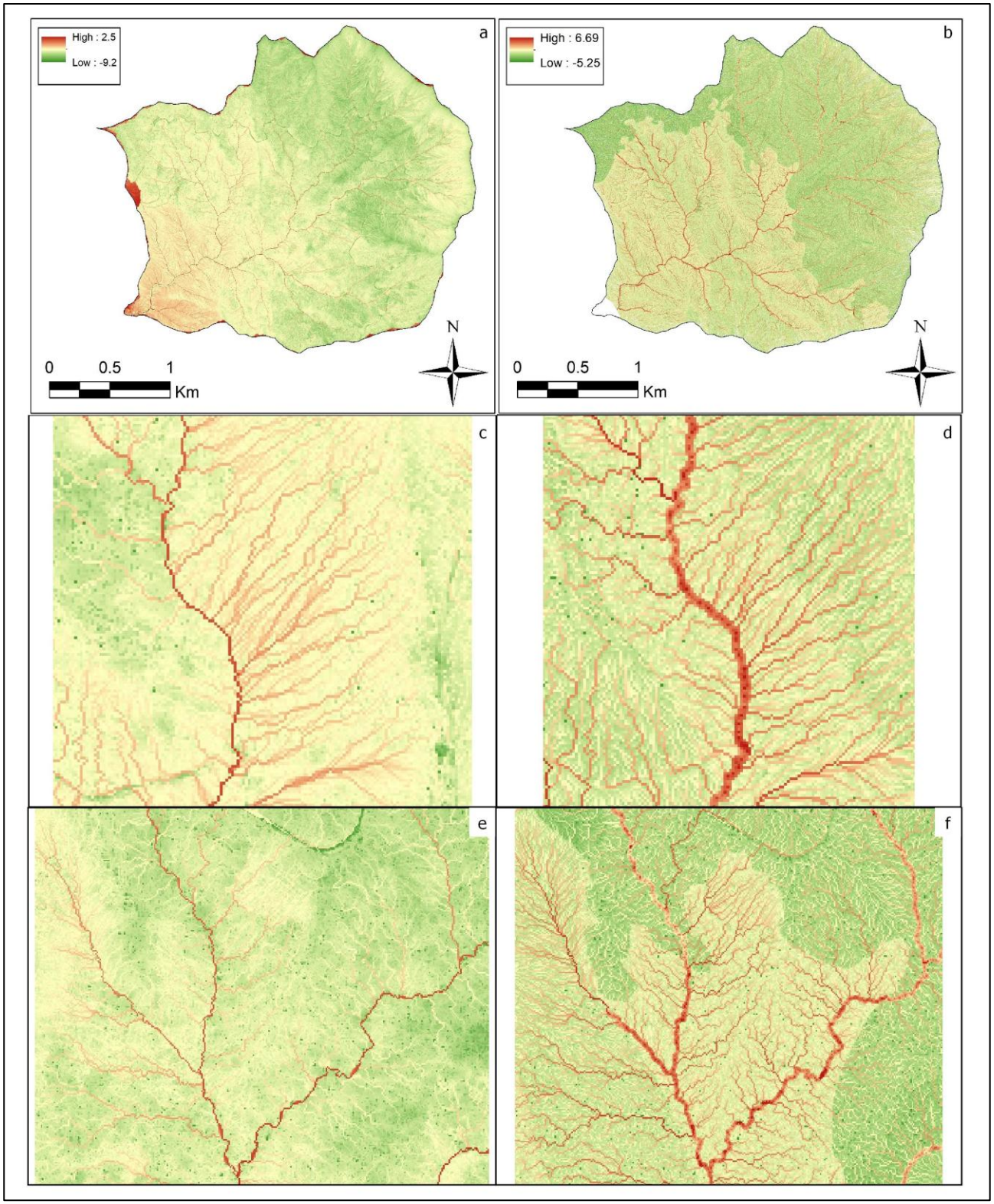

Figure 6. Comparison between IC index (**a**) and SCI index (**b**) maps. Panels **c** and **d** show a detailed map highlighting differences in contrasting flow values on the water courses w.r.t. surrounding hillslopes (IC and SCI, respectively). Panels **e** and **f** show another detailed map with differences in flow continuity (IC and SCI, respectively). See text for further discussion.

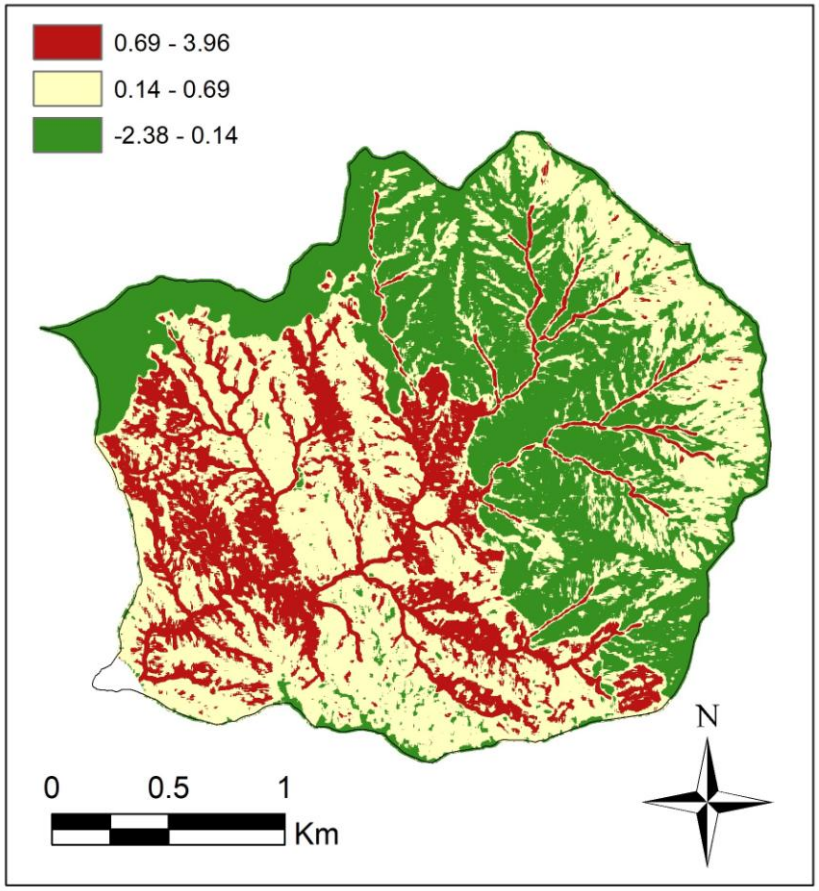

Figure 7. SCI map of the Vernazza basin after postprocessing, i.e., application of the mean filter and classification into 3 classes.

Tables

Rainfall (MAP) (mm per year) Minimum: 1100 → 0 Maximum: 1500 → 1	Rainfall values
1100 mm	0
1200 mm	0.25
1300 mm	0.50
1400 mm	0.75
1500 mm	1

Table 1. Mean Annual Precipitation (MAP) in the Vernazza catchment classified as rainfall values. The entire range (from maximum to minimum values of the temporal series) has been rescaled from 0 to 1 (see text for details).

Engineering geological units	Soil Stability Values
Sandstone/Terraced	0.25
Pelitic/Terraced	0.50
Sandstone/Wild	0.75
Pelitic/Wild	1

Table 2. Engineering geological units classified as soil stability values (see text for details).

Land use classes	Land use values
Urban areas	0
Grassland	0.2
Forest	0.4
Cultivated terrace	0.6
Abandoned terrace	0.8

Table 3. Land use classes and values associated in relation to sediment mobility (see text for details).

Graphical abstract

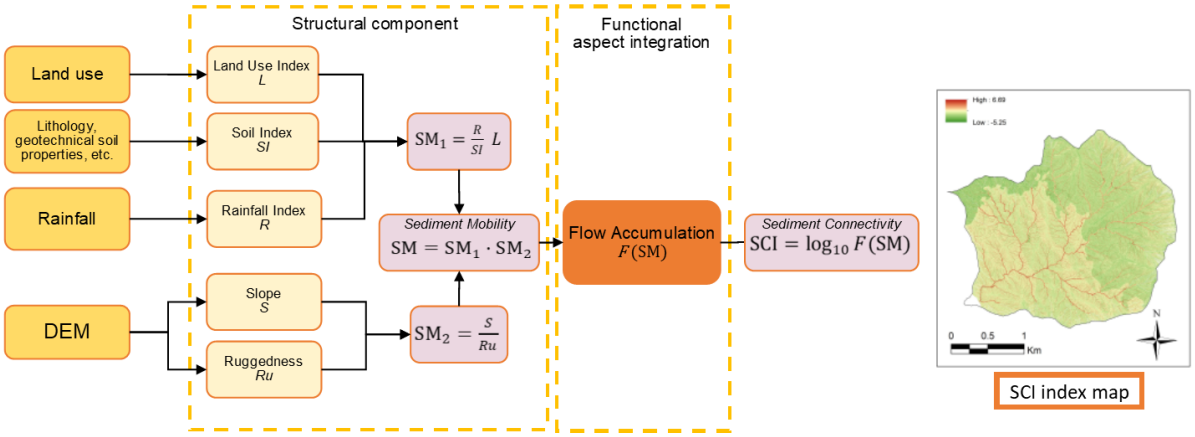

Highlights:

- A new mapping approach to sediment connectivity is presented.
- The approach models functional and structural components for sediment flow.
- Performance of the method is assessed on a test site in North-eastern Italy.
- New method has potential to be used in other catchments worldwide.